VI International Conference on Computational Methods in Marine Engineering
MARINE 2015
F. Salvatore, R. Broglia and R. Muscari (Eds)

MULTIDISCIPLINARY DESIGN OPTIMIZATION OF A SAILPLAN

Daniele Peri[1], Nicola Parolini[2], Fabio Fossati[3]
e-mail: d.peri@iac.cnr.it

[1] CNR-IAC - Istituto per le Applicazioni del Calcolo "Mauro Picone"
[2] MOX, Dipartimento di Matematica, Politecnico di Milano
[3] Department of Mechanics, Politecnico di Milano

Key words: Multidisciplinary Design Optimization, Global Optimization, Fluid-Structure Interaction, Sail Design.

Abstract. In this paper, multi-disciplinary optimization techniques are applied to sail design. Two different mathematical models, providing the solution of the fluid-dynamic and the structural problems governing the behaviour of a complete sailplan, are coupled in a fluid-structure interaction (FSI) scheme, in order to determine the real flying shape of the sails and the forces acting on them. A numerical optimization algorithm is then applied, optimizing the structural pattern of the sailplan in order to maximize the driving force or other significant quantities.

1 Introduction

Many real-life engineering problems couple different disciplines together. The numerical solution of the complete problem requires the availability of a mathematical model for each discipline and to account for the mutual interference effects: this activity is typically referred to as *multi-disciplinary design analysis* (MDA). Among *fluid-structure interaction* (FSI) problems (which represent a particular class of MDA), sail design is one of the most interesting, since the shape of the very flexible sail under load is heavily influenced by the wind flow field, which, in turns, changes as the shape of the sail is deformed. The structure of the sails (width, reinforcements, etc.) reacts under loads determining its final deformed shape, which is referred to as the *flying shape*. As a consequence, two embedded problems, aerodynamic and structural, need do to be solved together. Suitable FSI algorithms can be devised to predict the equilibrium solution between the aerodynamic loads and the structural response.

An additional level of computational complexity appears when looking for the *optimal shape* (with respect to a given performance index). In this case, a large number of MDA problems has to be solved in order to obtain the optimal solution: this is typically referred

to as *multi-disciplinary design optimization* (MDO). Each discipline contributes with its proper design variables and constraints, and the optimization is performed with respect to all the involved design variables. A prerequisite is obviously represented by the availability of a design tool able to solve the basic FSI/MDA problem.

In this paper, an inviscid aerodynamic solver (based on a potential flow model) is coupled with a finite element structural solver for the solution of the FSI/MDA sail problem. This tool is validated using proper wind tunnel data for a sail-plan composed by mainsail and jib [4]. The FSI solver is then integrated into an optimization framework. The adopted design optimization scheme, based on the Perttunen algorithm [10], allows an efficient exploration of the design variable space towards the optimal configuration.

The results of the MDO for a sail-plan are presented and discussed. In order to reduce the number of the design variables, only the structural properties of the sails are considered as unknown of the full MDO problem, while the initial sail shapes are not changed. However, other variables such as, *e.g.*, the sail trimmings, could also be accounted for by the proposed optimization strategy.

2 Numerical solvers

In this section, we briefly introduce two numerical solvers which are adopted for the solution of the fluid-dynamic and structural problems and the FSI scheme used to account for the aero-structural coupling.

2.1 Fluid-dynamic solver

We consider a sailplan for windward (upwind) sailing, composed by a mainsail and a jib. This configuration has been recently tested in the wind tunnel of *Politecnico di Milano*, collecting both sail forces and deformations in different flow conditions [4], that is a good validation dataset for assessing the accuracy of the FSI simulations.

Focusing the analysis on upwind sail configurations allowed us to simplify the physics that should be captured by the fluid-dynamic solver. In fact, the hypotheses of non-separated flow and thin wake (with prescribed separation lines) are applicable to the considered sailplan under these particular operating conditions, thus a potential flow solver can be used.

The adopted fluid-dynamic solver is based on the Vortex-Lattice Method (VLM) [7]. This approach is particularly suitable for thin bodies moving at high Reynolds number, where compressibility effects are negligible and the thickness of the boundary layer is small.

The present implementation has been developed in [8] and [9]. Here the vortex wake is initialized from known edge points, where the *Kutta condition* is enforced. The dynamic of the wake is not considered, and a *horseshoe-like vortex* is detaching from each corresponding panel of the body [6]. This technique has been proven to be fairly accurate for the prediction of integral quantities in case of flows around thin bodies [9], while the

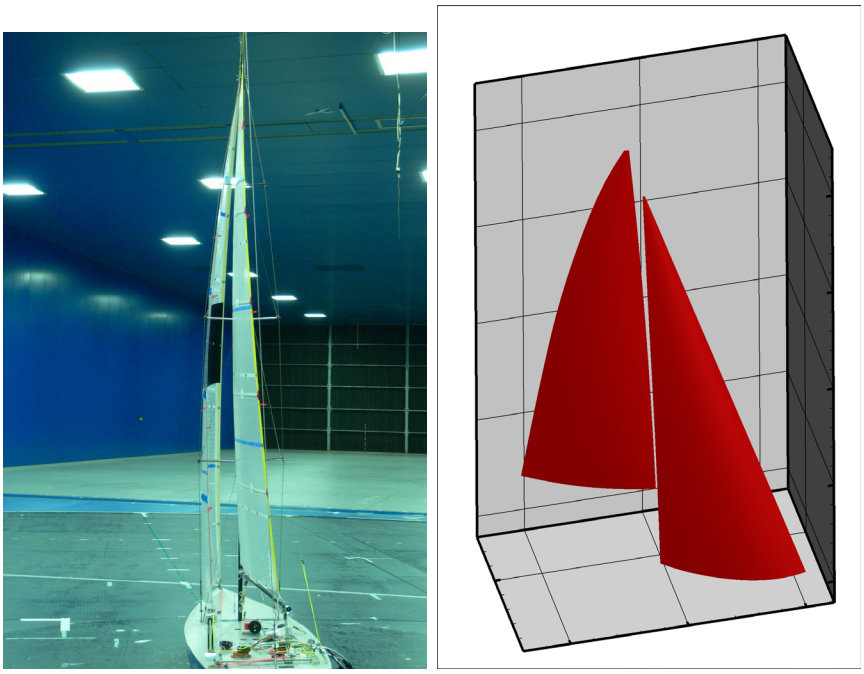

Figure 1: Sailplan model in the wind tunnel (left) and correspondent CAD reconstruction (right).

simplification on the computation of the nonlinear wake roll-up has a relevant effect in the reduction of the computational time.

2.2 Structural solver

An open-source finite elements code has been used for computing the sail deformation. The CalculiX code [1] can manage a large number of different structural elements. It has been largely validated with experiments and also by comparisons with other popular packages [3].

In this work, sail simulations are performed using shell elements with reduced integration. The same mesh as for the fluid-dynamic computations is adopted, in order to easily exchange the pressure and deformation data between the two codes. Structural properties of the sails have been obtained by a set of dedicated tension tests.

2.3 Aero-structural coupling

In the problem at hand, we are only interested in the final flying shape and a loosely coupled FSI scheme can be adopted. Since the computational grid is shared between the codes, the pressure values computed by the fluid-dynamic solver are simply applied to the corresponding panel of the structural grid. Conversely, the displacement of the grid nodes are transmitted to the grid of the fluid-dynamic solver. In order to improve the

stability properties of the FSI coupling, a relaxation procedure on the displacement may be adopted.

Convergence of the iterative procedure is controlled through the current value of the aerodynamic efficiency of the sailplan, that is, the ratio of the side force and the driving force: convergence is reached when the variation of the efficiency between two successive iterations is lower than $10^{-2}\%$. The use of the aerodynamic coefficient is a conservative choice, since it depends on two different aerodynamic quantities, so that convergence of both is implicitly required in order to have convergence of the FSI.

3 FSI test case

A first simulation has been produced for one of the experimental set-up analyzed in [4]. The adopted sailplan is reported in figure 1.

Some simplifications with respect to the real experimental configuration have been adopted. Firstly, only the sails are considered, while the hull is not modeled, as well as the entire rig. Secondly, since the mast is not included into the simulation, the deformation of the mast (which is small when compared to the sail displacement) is not considered, so that the leading edge of the mainsail is kept fixed. The forestay is modeled as a beam, and the leading edge (luff) of the jib is attached to it. The extremes of the forestay are constrained to fixed positions, while rotations are allowed. At last, the extreme aft point of the lower corner of the jib is positioned according to the sail trimming applied during the tests.

For the simulations, we have considered the experimental condition with apparent wind direction of 22 degrees and maximum driving force. The vertical speed profile has been measured in the wind tunnel and it is applied as a boundary condition in the fluid-dynamic solver. Numerical results in terms of driving (F_x) and side (F_y) forces are reported in table 1. Here a convergence analysis has been produced performing computations on three different grid levels, each obtained doubling the density of the previous level. Coarse grid is made by 5 panels along the short edge of the sail, 15 along the longer edge, being the number of panels the same on jib and mainsail. The other grids are obtained by doubling these numbers.

	F_x	F_y
Coarse grid (6 x 32)	0.162	0.864
Medium grid (11 x 63)	0.180	0.931
Fine grid (21 x 125)	0.186	0.961
Convergent value	0.188	0.972
Experiments	0.188	1.483
Percentage difference	0.000	34.474

Table 1: Numerical and experimental force values for a sailplan configuration.

The difference between the predicted value on the driving force and the experimental data is below 1%, while for the side force the difference is increased up to 34%. These values are encouraging, in particular if we consider the simplicity of the adopted fluid-dynamic model. Similar results are also obtained in [5] on the same sailplan and with a similar FSI model. The fact that the asymptotic value of the driving force is equal to the experimental value cannot be assumed as a proof of the predictive qualities of the fluid-dynamic code, but it must to be observed in conjunction with the associated precision index. In fact, convergence study of the FSI procedure allows to fix the confidence interval of the fluid-dynamic quantities here observed [2]. For the driving force, the validation uncertainty is 2.4% while for the side force it is 3.6%. As a consequence, the intrinsic precision of the numerical solver is fixed at these levels, and the optimization procedure can be considered affordable if the objective function is reduced of a quantity larger than the precision index of the code.

The uniqueness of the convergent solution for the flying shape cannot be proven for this really complex problem. For this reason, the adoption of a relaxation factor can be used in order to ensure the convergence to a stable solution: once the sail deformation is computed, the shape variation is not applied completely to the current shape before a new fluid dynamic evaluation of the loads is performed, but a fraction of it is applied, so that the convergence to the final shape is slower. The first implication of this practice is the increase of the number of iterations required for a complete convergence, and a linear increase of the computational time. The results obtained for the FSI problem at hand, with and without the application of a relaxation factor for the sail deformation, are reported in figure 2. In this picture, at each step of the iterative procedure, the percentage difference between the value of the aerodynamic efficiency and the average of the final values obtained with and without the use of a relaxation parameter is reported. Final difference is lower than 10^{-1}%, that is, the difference between the convergent value provided by the FSI scheme with and without the application of a relaxation parameter is largely lower than the precision limit of the adopted fluid dynamic solver: as a consequence, the use of a relaxation parameter is not producing significative differences on the convergent results.

In the case of the application of the full deformation, only 7 iterations are needed in order to reach a convergent value of the aerodynamic coefficient of the sailplan. On the contrary, if a relaxation factor of 0.25 is applied, the number of iterations is increased to 27. However, the convergent value of the aerodynamic efficiency differs of around 0.1%. This value is absolutely lower than the measured precision index, so that the optimization will be performed without the application of a relaxation factor.

The limited number of iterations required to achieve convergence and the moderate computational time required for the overall solution of the coupled FSI problem do not call for the adoption of particular techniques for the relaxation of the convergence, typically adopted in MDO: a full multidisciplinary design analysis will be performed during the following optimization study every time the solution of the FSI problem is required.

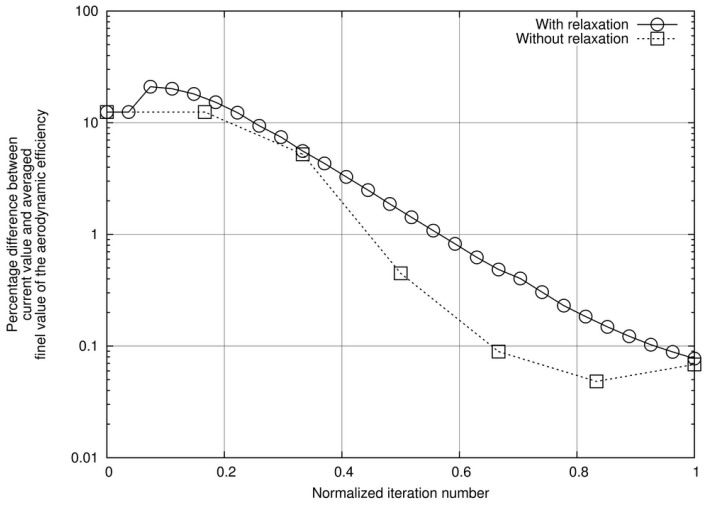

Figure 2: Effect of the adoption of a relaxation parameter for the sail deformation. On the horizontal axis, the iteration number normalized by the corresponding maximum number. On the vertical axis, the aerodynamic efficiency normalized by the average of the convergent values obtained with the two methods. Relaxation factor: 0.25.

4 Optimization approach

The FSI test presented in the previous section shows that the numerical models adopted for the solution of the FSI problems can guarantee an acceptable level of accuracy. The key result of the present work is the integration of the FSI scheme in an optimization framework. The design parameters that we consider in the optimization are related to the structural properties of the sails, while their initial shapes are not changed (although the initial shapes are then deformed during the FSI iteration). In the following, the various elements of the optimization problem are illustrated.

4.1 Structural parameterization

The solution of an optimization problem requires to define a parametric model of the object we want to optimize. Since the sailplan is described by a finite number of rectangular panels, the simpler and more intuitive idea could be to assign a different value of the mechanical properties to each mesh element. In this way, hundreds of design variables for each sail would be required.

In order to reduce the number of unknowns of the optimization problem, we should observe that:

1. preliminary tests have demonstrated how, considering a plausible range of local variation of the mechanical properties of the sails (induced i.e. by varying the thickness), the deformation of the mainsail is not changing that much. This is probably due to the stiffness of the constraints, since two sides of the mainsail are

rigidly fixed to the boom and the mast.

2. An excessive local variation of the structural properties can hardly be manufactured, while a pattern of local variations obtained by a number of reinforcements applied on the sail is much more reasonable. This is, by the way, the usual approach adopted by sailmakers.

As a consequence, the mainsail is not considered during the optimization procedure, and its structure is preserved. Local thickness of the jib is modified along a number of prescribed patterns: variation of the thickness is constant along the pattern, and the thickness modification for a single pattern represents a design variable for the problem.

4.2 Optimization algorithm

In principle, the selected parametric model for the structure of the jib allows to increase or decrease locally the thickness of the sail. However, a reduction of the thickness may threaten the overall strength of the sail: in order to preserve integrity, we assume that the thickness of the sail cannot be reduced more than one half of its initial value. On the other hand, we want also to avoid a too large increment of the local thickness, so that the local thickness is limited in between one half and the double of the original thickness of the sail.

The presence of lower and upper bounds for the values of the design variables, and the limited number of design variables, suggest the use of the Perttunen algorithm [10]. This algorithm considers the portion of space bounded by the hyper-hexahedron defined by the upper and lower limits of the design variables, and then it proceeds by successive subdivisions of the original interval, producing an extensive partitioning of the assigned portion of space, and focusing on the more promising regions.

The algorithm is initialized by computing the objective function on the corners of the overall interval, and then subdividing the space by using a suitable partitioning techniques, i.e. Delaunay triangularization. The space is now divided into a limited number of sub-intervals, defining a convex hull.

At each iteration, one of the current intervals is selected for refinement. Selection of the interval is obtained basing on the rank of the objective function at each corner of the interval, selecting the interval minimizing the functional

$$A_{min} = \prod_{j=1}^{ndv+1} R^{(i_j)}/V \tag{1}$$

The position for the evaluation of the new value of the objective function is selected as

$$x^{(i)} = \frac{\sum_{j=1}^{ndv+1} x^{(i_j)}/R^{(i_j)}}{\sum_{j=1}^{ndv+1} 1/R^{(i_j)}} \tag{2}$$

once the subdividing interval is detected. Evaluation of the volume of the interval is performed by computing the determinant of the matrix $|V|$

$$V = \begin{vmatrix} x_1^{i_{s,1}} x_1^{i_{s,ndv+1}} & \dots & x_{ndv}^{i_{s,1}} x_{ndv}^{i_{s,ndv+1}} \\ \dots & \dots & \dots \\ x_1^{i_{s,ndv}} x_1^{i_{s,ndv+1}} & \dots & x_{ndv}^{i_{s,ndv}} x_{ndv}^{i_{s,ndv+1}} \end{vmatrix}.$$

Once a new point is added, a new Delaunay triangularization is produced, and a new iteration is performed. The algorithm stops when the volume of the larger interval is below a prescribed value, or if there is not a further reduction of the objective function for a certain number of iterations. In the following applications, 1000 iterations were usually sufficient for the convergence of the algorithm.

5 Numerical optimization results

Here the Perttunen algorithm is applied to the maximization of the aerodynamic efficiency of the previously described sailplan. In order preserve the sideforce generated by the sailplan to contrast the wind action, an equality constraint on the sideforce is applied, and a linear penalty is added to the objective function. The equality constraint is applied because here we are not modeling the submerged part of the yacht, so that we have to assume the same behaviour of the sailplan for what is concerning the equilibrium of the sailboat. For the same reason, a variation of the leeway angle in order to preserve the side force has been not considered.

A series of five different patterns for the reinforcements of the jib have been utilized, and they are reported in figure 3. They have been produced observing the results from a number of preliminary problem.

The first pattern (P3A) is composed by three reinforcements starting from the corners of the sail and converging in the central part. An increase of the driving force of about 4.103% is predicted, with a constant side force. There is a small increase of the heeling moment (0.240%) The effect of the vertical reinforcement has been observed to be very limited, so that it has been removed in the P3B pattern, and substituted with a reinforcements connecting the lower corners of the jib.

Results of P3B represent an improvement with respect to P3A. Increase of the driving force is here 7.149% while the side force is increased a little (0.721%). Small variations are possible due to the application of a quadratic penalty. The increase of the heeling moment is moderate (0.481%). In general, the tendency is to produce a sail more rigid in the front part and softer in the aft part, as it can be observed in figure 4.

With P4A pattern, the vertical reinforcement has been reintroduced, preserving the same scheme of P3B. Results are absolutely identical to the ones from P3B. As a consequence, the pattern has been modified by splitting the fore reinforcement. No further improvements have been obtained by using the P4B pattern.

The final results of the optimization can be regarded as a real improvement of the initial configuration, since the improvements obtained are larger than the uncertainties

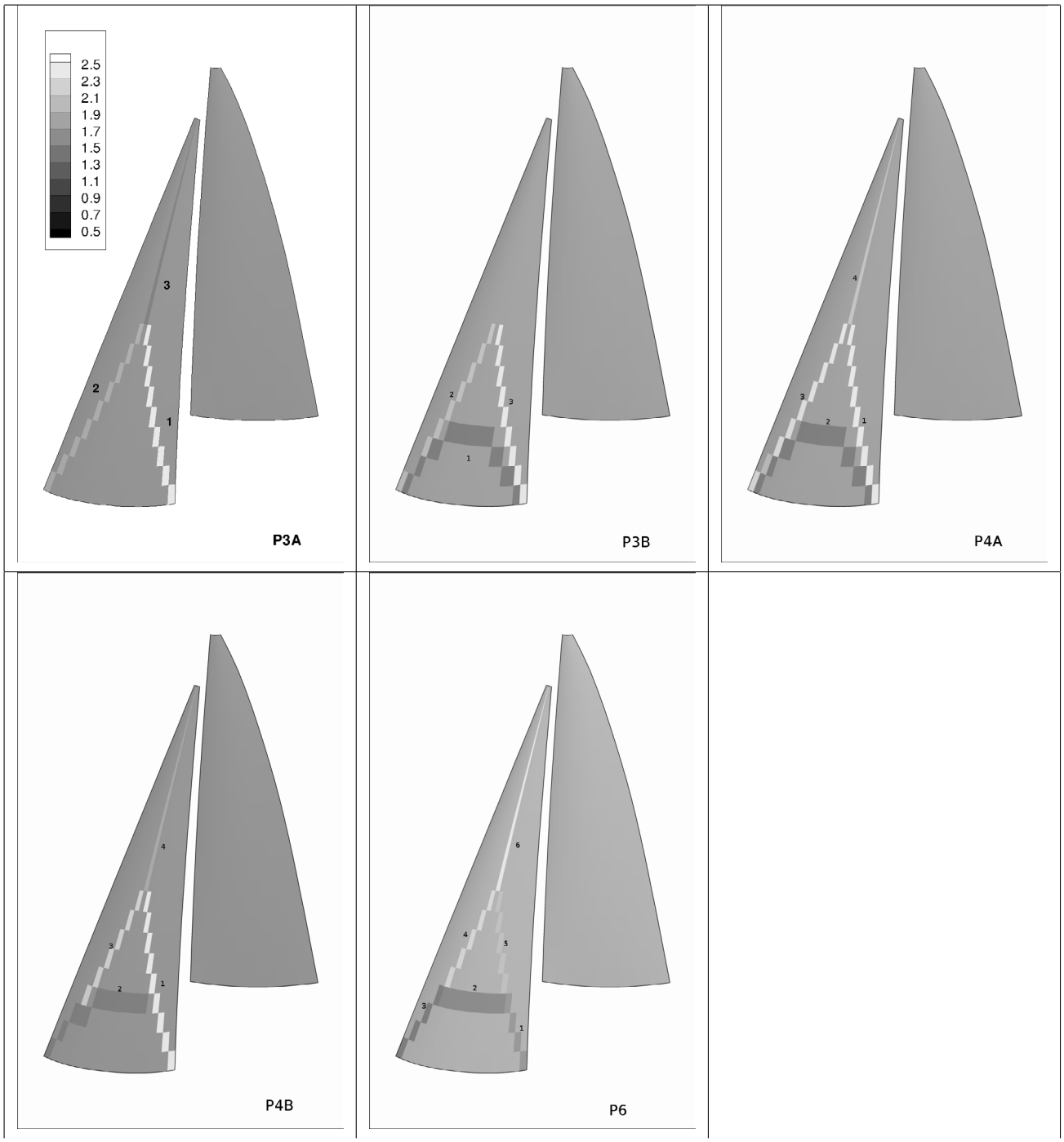

Figure 3: Different patterns adopted for the jib reinforcements: different gray scales represent the reinforcements, numbers indicating the design variable. From left to right, top to bottom, schemes P3A, P3B, P4A, P4B, P6. Grayscale is indicating the ratio between the local thickness and the original (uniform) thickness.

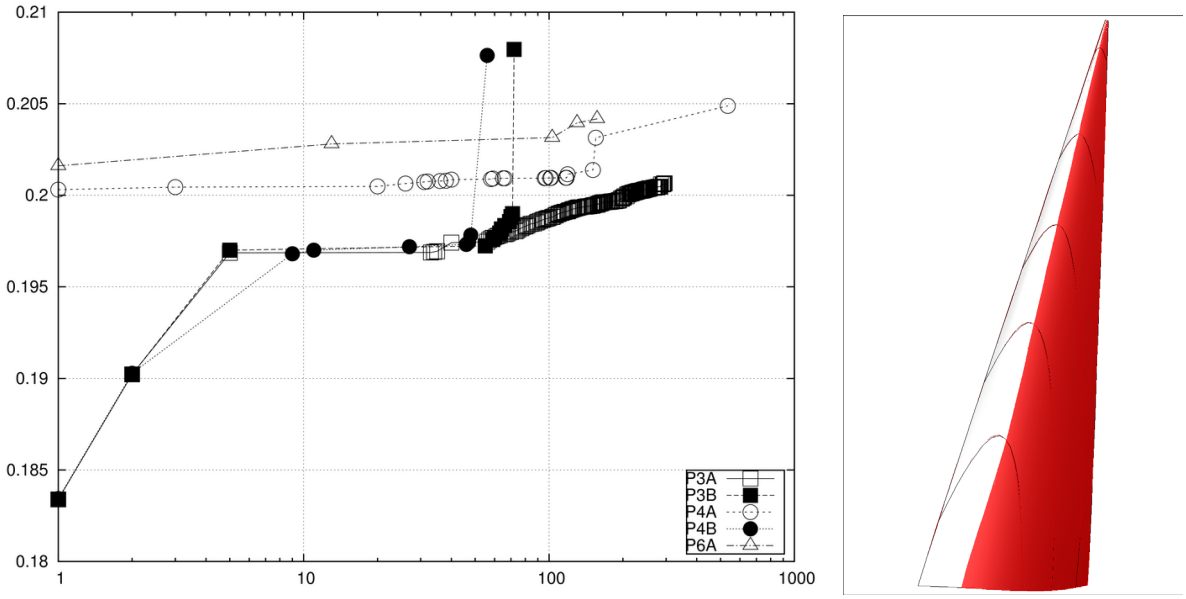

Figure 4: Evolution of the best value as a function of the iteration number for the different parametric models of the jib (left). Side view of the original and optimal flying shapes (right). Dark region indicates that the optimal shape is closer to the observer, while white region is indicating the opposite.

associated to the numerical solver estimated by the convergence analysis reported in table 1.

An increase of the driving force of about 7% represents an improvement of paramount importance, in situations where an increase of about 1% may discriminate between wining or loosing a competition. A dedicated experimental activity would be obviously necessary for a complete validation of the procedure.

6 Conclusions

In this paper, we have presented the multi-disciplinary design optimization of a sailplan which accounts for the deformation of the sails through the solution of a fluid-structure interaction problem. For the specific (upwind) flow conditions considered in this work, a potential flow solver has been adopted allowing for a fast solution of the fluid-dynamic problem. Moreover, just a few iterations were enough to reach the equilibrium configuration in the FSI problem. Combining this computational efficiency with the fast exploration of the design variable space guaranteed by the Perttunen optimization algorithm enabled us to obtain a valuable numerical tool for the solution of the complex MDO problem.

Optimal solution of the problem shows an improvement of the overall performances whose value is evidently larger than the precision limit of the fluid dynamic solver, so that numerical improvements are credible. Performance increase is of great importance in the spite of application to competitions, where few percentage points may represent the difference between winning and loosing a race.

Optimizing not only the reinforcements but also the shape of the initial sail geometry may represents a further step toward a complete optimization of the sailplan, as well as the adoption of a more complex fluid dynamic solver.

REFERENCES

[1] Dhondt G., 'CalculiX CrunchiX USERS MANUAL version 2.8p2', http://www.calculix.de/

[2] Coleman H.W., 'Uncertainty Considerations in Validating CFD Codes with Experimental Data', AIAA Paper 96-2027, 27^{th} AIAA Fluid Dynamics Conference, New Orleans, LA, June 17-20 1996.

[3] Dhondt G., 'The Finite Element Method for Three-Dimensional Thermo mechanical Applications', Wiley, Hoboken 2004, ISBN 0-470-85752-8

[4] Fossati F., Muggiasca S., Martina F., 'Experimental database of sails performance and flying shapes in upwind conditions', in *Proceedings of International Conference Innovation in High Performance Sailing Yachts*, Lorient, France, ISBN: 978-1-905040-46-9, 29-30 May 2008.

[5] Helmstad, R., Larsson, T., 'An Aeroelastic Implementation for Yacht Sails and Rigs', Degree project in Naval Architecture, KTH Engineering Science, Stockholm, Sweden 2013.

[6] Inoue S., 'On the turning of ships', The memoirs of the Faculty of Engineering, Kyushu University, 1956.

[7] Katz J., Plotkin A., 'Low-Speed Aerodynamics - From Wing Theory to Panel Methods', McGraw-Hill Series in Aeronautical and Aerospace Engineering, 1991.

[8] Landrini M., Casciola C.M., Coppola C., 'A Non-Linear Hydrodynamic Model for Ship Maneuverability', in *Proceedings of International Conference on Marine Simulations and Ship Maneuverability* (MARSIM '93), St. John's (Newfoundland - Canada), 1993.

[9] Peri D., 'Un modello a vortici per la manovrabilitá delle navi', M.Sc. "La Sapienza" University, 1994.

[10] Perttunen C.D., 'Computational geometric approach to feasible region division in constrained global optimization', in *Proceedings of the 1991 IEEE Conference on Systems, Man, and Cybernetics*, IEEE, 1991.